Correlation between the interlayer Josephson coupling strength and an enhanced superconducting transition temperature of multilayer cuprate superconductors

Y. Hirata, K. M. Kojima, M. Ishikado, and S. Uchida
Department of Physics, University of Tokyo, Hongo 7-3-1, Bunkyo-ku, Tokyo 113-0033, Japan

A. Iyo and H. Eisaki
National Institute of Advanced Industrial Science and Technology (AIST), Tsukuba Central 2, Umezono 1-1-1, Tsukuba, Ibaraki 305-8568, Japan

S. Tajima
Department of Physics, Osaka University, Machikaneyama 1-1, Toyonaka, Osaka 560-0043, Japan
(Received 12 June 2011; revised manuscript received 16 November 2011; published 2 February 2012)

Infrared reflectivity spectra of multilayered $HgBa_2Ca_{n-1}Cu_nO_{2n+2+\delta}$ ($n = 2, 3, 4$, and 5) are measured. Optical plasma modes associated with the Josephson coupling between CuO_2 planes within a multilayer appear below T_c in the c-axis component of the reflectivity spectrum. The result allows for quantitative estimation of the interlayer Josephson coupling strength within a multilayer. It is found that the change of the Josephson coupling strength correlates with the increase of T_c up to $n = 3$ and the subsequent decrease for $n \geqslant 4$.

DOI: 10.1103/PhysRevB.85.054501 PACS number(s): 74.25.Gz, 74.50.+r, 74.62.Yb, 74.72.−h

I. INTRODUCTION

There are several factors which influence T_c of high-T_c superconducting cuprates. It is well known that T_c is predominantly determined by the carrier doping level, or somehow related to the superfluid density ρ_s.[1] It is also known that T_c is influenced by some other factors, such as the apical-oxygen distance from the CuO_2 plane[2] and the number of CuO_2 planes, n, in a unit cell in the multilayer cuprates.[3,4] These two probably make T_c material-dependent. The multilayer effect surely exists in the cuprates and enhances T_c with respect to T_c of single-layer cuprates up to $n = 3$, but its mechanism is not well understood.

The interlayer tunneling theory (ILT)[5] is one of the proposals which try to explain the rise of T_c with n. According to ILT, the tunneling of Cooper pairs between the planes via Josephson coupling gains the kinetic energy along the c axis (perpendicular to the planes), which promotes the pairing of quasiparticles and drives superconductivity. In the framework of the ILT model, $T_c(n)$ of the n-layer cuprate is an increasing function of n due to additional Josephson coupling between the CuO_2 planes within an n layer:

$$T_c(n) = T_c(1) + C\left(1 - \frac{1}{n}\right), \tag{1}$$

where C is a certain constant.[6] Leggett derived exactly the same expression by taking into account the interplane Coulomb interaction.[7]

However, a serious problem with ILT is that for single-layer cuprates the interlayer Josephson coupling is found not to be strong enough to account for the superconducting condensation energy.[8,9] Another difficulty is that in multilayer cuprates T_c decreases for $n \geqslant 4$. NMR experiments[10,11] have revealed that the hole concentration in the inner planes (IP) is significantly smaller than that in the outer planes (OP). It is argued that the decrease in T_c is due to this doping imbalance which tends to induce some competing order in the IPs.[12]

The c-axis optical measurement allows us to directly observe Josephson coupling between CuO_2 planes in high-T_c superconductors. The strength of interlayer Josephson coupling can directly be estimated from the frequency of the so-called Josephson plasma mode showing up as a reflectivity edge in the c-axis spectrum below T_c.[13] Van der Marel and Tsvetkov predicted that there would appear additional modes, called optical Josephson plasma modes, in the c-axis optical response of the cuprates which would consist of an alternating stack of more than one kind of Josephson junctions.[14] A bilayer cuprate is thought to be a typical example with a stronger junction within the bilayer and a relatively weak junction between bilayers. In $YBa_2Cu_3O_{7-\delta}$ (YBCO) and $Tl_2Ba_2Ca_2Cu_3O_{10+\delta}$ (Tl-2223) an optical mode appears at relatively high frequencies, 400–500 cm^{-1},[15–19] probably reflecting strong coupling between closely spaced CuO_2 planes within bi- and trilayers, although other explanations are suggested for the origin of this mode.[20]

Here we report the first systematic optical measurement carried out for the multilayer systems. The optical Josephson plasma modes are observed in the reflectivity spectra of Hg-based multilayer cuprates, $HgBa_2Ca_{n-1}Cu_nO_{2n+2+\delta}$ [Hg-12($n-1$)n] for n from 2 to 5. The result reveals how the interlayer Josephson coupling strength within a multilayer varies with n, which makes it possible to address the basic questions concerning the multilayer cuprates: (i) why does the multilayer structure enhance T_c, (ii) what is the effect of the charge imbalance between inner and outer planes, and (iii) why is T_c highest in Hg-based cuprates?

II. EXPERIMENTS

Since single crystalline samples of multilayered Hg-based cuprates with sufficiently large thickness along the c axis are difficult to grow, we used polycrystalline samples for the optical measurement. High-density ceramic samples were synthesized using a cubic-anvil high-pressure synthesizing

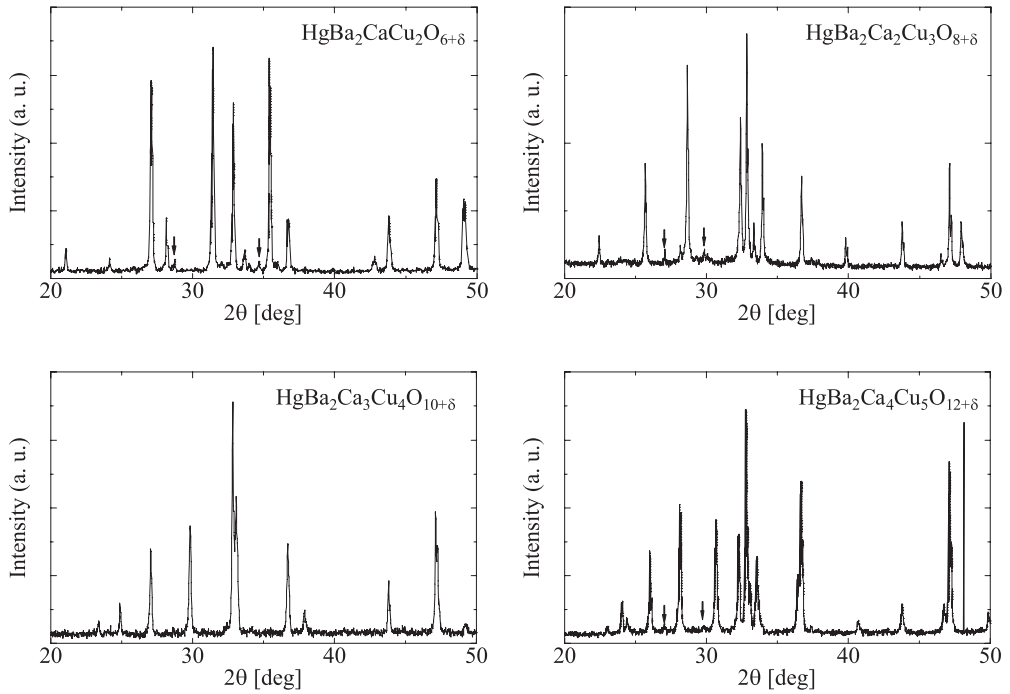

FIG. 1. The x-ray diffraction patterns of (a) Hg-1212, (b) Hg-1223, (c) Hg-1234, and (d) Hg-1245. Solid arrows indicate impurity signals.

apparatus.[21,22] The precurser is prepared by mixing powder samples of BaO_2, Ca_2CuO_3, and Cu, heating them for 12 h at 900 °C under O_2 flow, and annealing them for 2 h at 800 °C under N_2 flow. HgO, CuO, Cu, and the precursor are mixed and pressed into a pellet, sealed in a Au capsule, and then sintered for 2–4 h at 700–1000 °C under the pressure 3.5–4.5 GPa. Figures 1(a)–1(d) show x-ray powder diffraction patterns of sintered samples. The impurity phase fraction of each sample was less than 5%. Since optical reflectivity is a bulk sensitive probe, the contribution from the 5% minor phase is utmost 5% in optical reflectivity and negligible. T_c determined by the dc magnetization measurement was 127 K for Hg-1212, 134 K for Hg-1223, 125 K for Hg-1234, and 103 K for Hg-1245, which are close to the highest T_c values ever reported and evidence that all the samples are optimally doped.[23,24]

The sample pellets were polished with Al_2O_3 powders until they had mirror surfaces for the optical measurement. Reflectivity spectra were measured in the frequency range between 50 and 4000 cm^{-1} and the temperature range from 4 K to 300 K using a Fourier-transform infrared spectrometer and a cryostat. The optical response of a polycrystalline sample is the mixture of the *ab* plane and the *c*-axis component. In the long wavelength limit, where the wavelength is much longer than the grain size, the reflectivity of the polycrystalline sample is an average of the reflectivity along each crystal axis. On the other hand, in the short wavelength limit, where the wavelength is overwhelmingly shorter than the grain size, the reflectivity of the polycrystalline sample represents the response of the effective medium.[25] Since the typical grain size of our sample is several micrometers, which is a little shorter than the wavelength at which the reflectivity is measured, neither limit is a good approximation. However, the *ab*-plane reflectivity spectra of single crystalline Hg-1201 and Hg-1223 are known to be featureless below 1000 cm^{-1},[26] so most of features appearing in the spectrum originate from the *c*-axis component. The polycrystalline reflectivity spectrum resembles the *c*-axis reflectivity spectrum in the shape and the frequencies of the features, although the absolute value of the polycrystalline reflectivity does not represent the actual *c*-axis reflectivity.

In order to observe an intermultilayer (acoustic) Josephson plasma mode at low frequency below 150 cm^{-1}, we performed the sphere resonance measurement.[27] The polycrystalline sample pellets were ground into grains $\sim$2 μm in diameter, mixed with polyethylene powder in a volume fraction of 3%, pressed into pellets, and heated at 140 °C. Then, transmission spectra of the composite pellets were measured in the frequency range between 20 and 150 cm^{-1} and the temperature range from 5 K to 300 K using a Fourier-transform infrared spectrometer and cryostat.

III. RESULTS

The reflectivity spectra at various temperatures for a series of multilayered samples are shown in Figs. 2(a)–2(d). Above 1000 cm^{-1} the spectrum is featureless and the reflectivity decreases monotonically (due to, for example, the light scattering from grain boundaries). In the reflectivity spectrum of the bilayer Hg-1212 [Fig. 2(a)] at $T = 300$ K, several features are observed which correspond to the optical phonon modes. Notably, the apical-oxygen stretching mode at 630 cm^{-1} and the planar-oxygen bending mode at 330 cm^{-1} are easily identified by comparing with the reported *c*-axis spectrum of single crystalline Hg-1201.[28] Below $T_c = 127$ K a broad peak centered at 800 cm^{-1} develops which is thought to be an optical Josephson plasma mode. This frequency is distinctively higher

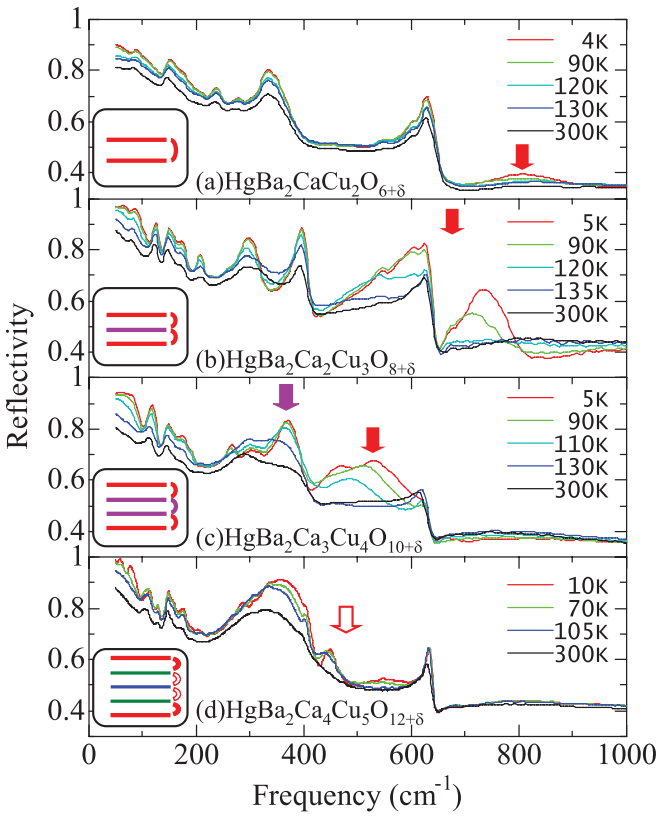

FIG. 2. (Color) The reflectivity spectra of polycrystalline samples, (a) Hg1212, (b) Hg1223, (c) Hg1234, and (d) Hg1245, at several temperatures below and above T_c. The spectrum just above T_c of each sample is displayed by the dark-blue curve. Red and purple arrows indicate the positions of the optical Josephson plasma modes determined by the analysis shown in Fig. 3. The corresponding Josephson couplings are depicted schematically in the insets.

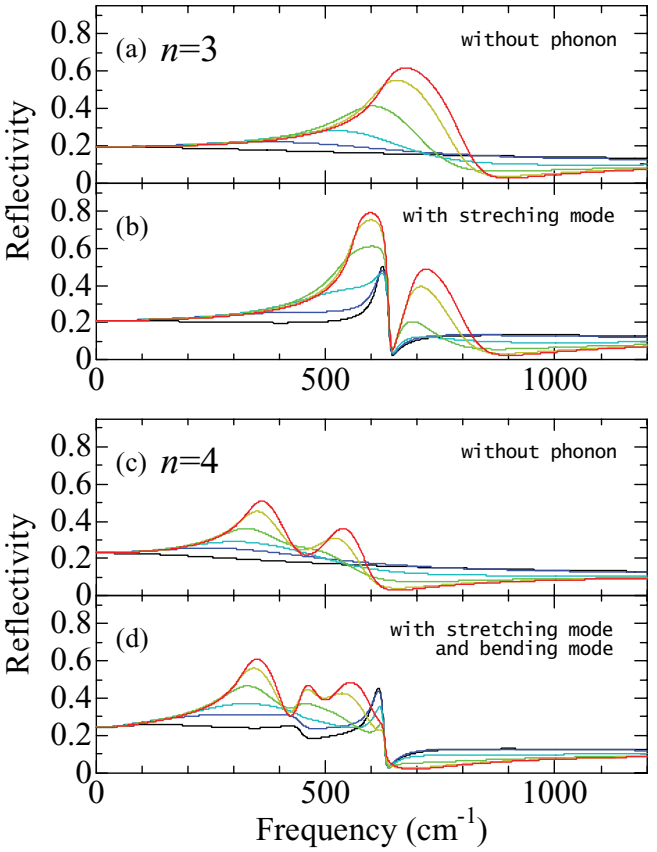

FIG. 3. (Color) Simulation of the observed reflectivity spectra using the scheme by Munzar *et al.*[29,30] in the presence of optical phonon modes which couple with the optical Josephson plasma modes. (a) The reflectivity spectrum of a three-layer system where one optical Josephson plasma resonance mode is located at $\tilde{\omega}_p \sim 800$ cm^{-1} without an optical phonon mode nearby. (b) The reflectivity spectrum of the same system with the 620 cm^{-1} apical-oxygen stretching mode. (c) The reflectivity spectrum of the four-layer system where two optical Josephson plasma modes exist at $\tilde{\omega}_{p1} \sim 640$ cm^{-1} and $\tilde{\omega}_{p2} \sim 480$ cm^{-1} without optical phonon modes. (d) The reflectivity spectrum of the same system with the apical-oxygen stretching mode at 620 cm^{-1} and the planar-oxygen bending modes at 390 cm^{-1}.

than the frequency of similar optical modes so far reported for other bi- and trilayer cuprates, indicating a strong Josephson coupling within a bilayer in Hg-1212.

The trilayer Hg-1223 has two inequivalent CuO_2 planes, two OPs and one IP, which make the oxygen bending mode split into two 300 and 400 cm^{-1} peaks in the spectrum of Hg-1223 [Fig. 2(b)]. The highest phonon (apical-oxygen mode) is seen at the same frequency ($\sim$620 cm^{-1}) as that in Hg-1212. Below $T_c = 134$ K, two bumps develop on both sides of the apical-oxygen mode. Since the trilayer is regarded as a series of two equivalent Josephson junctions [inset of Fig. 2(b)], there should be one optical Josephson plasma mode. We tried to reproduce the shape of this superconducting spectrum using the model used by Munzar *et al.*[29,30] Since the parameters for the apical-oxygen phonon mode are known from the spectra above T_c, there are only a few parameters in the model: the frequency of the Josephson plasma mode, and the background conductivity which damps the plasma mode. These parameters are temperature dependent, but we can make reasonable assumptions for their temperature dependencies—the plasma frequency increases reflecting the stronger Josephson coupling, while the background conductivity decreases associated with the opening of the superconducting gap, as the temperature is lowered. With this simple model, the qualitative features of the spectrum are very well reproduced as shown in Fig. 3(b). We see that the peak of the optical Josephson mode in Hg-1223 is much more pronounced than that in Hg-1212. This is probably because the plasma mode is located well inside the superconducting gap ($2\Delta_0 \sim 800$ cm^{-1} or even higher[31]) in Hg-1223, whereas the mode energy would be comparable with $2\Delta_0$ in Hg-1212, suffering damping from gap excitations. The optical Josephson plasma mode shows up at $T_p \sim 140$ K, slightly higher than T_c, which suggests that the intramultilayer phase coherence exists as the superconducting fluctuation while the intermultilayer phase coherence is lost above T_c.

The reflectivity spectrum of the four-layer Hg-1234 [Fig. 2(c)] shows complicated features developing below $T_c = 125$ K in the frequency range between 250 and 600 cm^{-1}. In the spectrum at 130 K the apical-oxygen mode is seen at 610 cm^{-1}, and the planar-oxygen bending modes and Ca-vibrational modes are in the range between 250 and 400 cm^{-1}. Below

T_c three bumps are developing at ~370, 460, and 530 cm^{-1}. Again, these features can be reproduced by assuming the plasma modes developing below T_c which couple predominantly with two bending phonons. To qualitatively reproduce the experimental spectral features below T_c, one needs to assume *two* optical Josephson modes at 360 and 540 cm^{-1} at T = 5 K [Fig. 3(c)]. Since the multilayer (four-layer) in Hg-1234 is regarded as a stack of two inequivalent Josephson junctions [inset of Fig. 2(c)], the appearance of two optical Josephson plasma modes is naturally expected. The higher-frequency mode probably corresponds to the Josephson coupling between IP and OP and the lower mode to the coupling between the two IPs. Then, by taking into account the coupling with the planar-oxygen bending phonons and the apical-oxygen phonon, a remarkably good agreement is obtained between the simulation [Fig. 3(d)] and the experimental result [Fig. 2(c)]. Note that the Josephson plasma frequencies appreciably decrease as compared with those in Hg-1212 and Hg-1223, probably because of low hole density in the IPs which would weaken the superconducting order[32] (or strengthen a competing order) and make the Josephson coupling weaker. The high-frequency optical plasma mode arises from $T_{p1} \sim$ 130 K, slightly higher than T_c, while the low-frequency mode seems to arise from $T_{p2} > 150$ K, much higher than T_c. This suggests that the phase coherence between underdoped IPs appears at higher temperature than between overdoped OPs and underdoped IPs, which is consistent with the measurement of the Nernst coefficient where the superconducting fluctuation appears at higher temperatures in underdoped samples than in optimally doped and overdoped samples.[33]

The superconducting response of the five-layer Hg-1245 (T_c = 103 K) is not so dramatic, and only appears as an enhanced reflectivity over a broad frequency range between 250 and 600 cm^{-1} [Fig. 2(d)]. The spectral features are expected to be similar to those in the spectrum of Hg-1234 [Fig. 2(c)], since the five layers in Hg-1245 are regarded as a series of two inequivalent Josephson junctions as in the case of the four layers in Hg-1234. We speculate that in Hg-1245 the superconducting order is weakened in the three IPs, which further weakens the interlayer Josephson coupling within a multilayer as compared with that in Hg-1234. This speculation is based on NMR experimental results for the same system.[11] All of the experimental results together with the successful simulation of the results for n = 3 and 4 give strong support for the interlayer Josephson coupling as the origin of the observed optical modes.

As regards the acoustic Josephson plasma mode associated with the intermultilayer Josephson coupling, it would show up as a reflectivity edge at low frequency also for the multilayer cuprate. For single-layer Hg-1201, it is observed at 70 cm^{-1} at T = 10 K in the c-axis spectrum of single crystalline Hg-1201.[28] However, for polycrystalline samples due to the dominance of the ab-plane component of the reflectivity in the low-frequency region, it is difficult to identify the Josephson plasma edge in the measured reflectivity spectrum. Nevertheless, it is possible to identify the acoustic mode using the sphere resonance method.[27] The results of the sphere resonance measurement are shown in Figs. 4(a)–4(d) which clearly identify the acoustic Josephson plasma mode as a dip in the spectrum below T_c. On the transmission

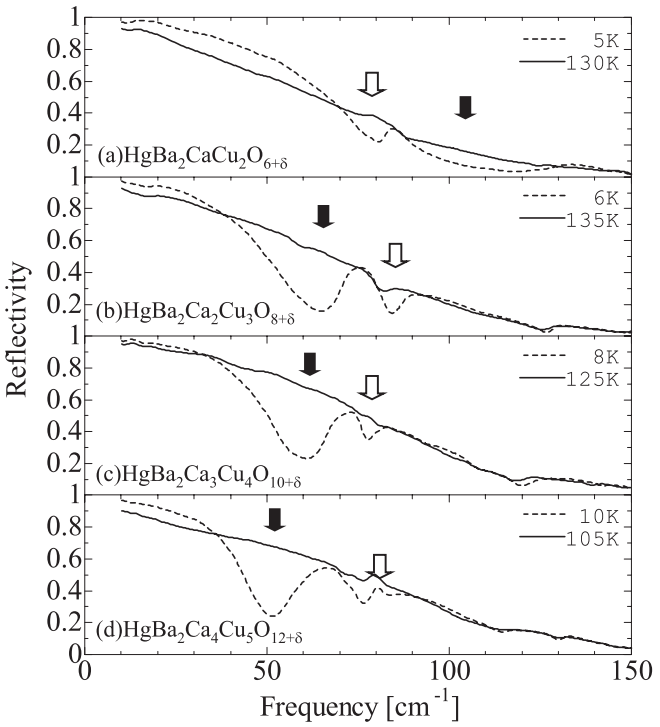

FIG. 4. The transmission spectra of (a) Hg-1212, (b) Hg-1223, (c) Hg-1234, and (d) Hg-1245. The spectrum at just above T_c and the lowest temperature of each sample are displayed by the solid curve and the broken curve, respectively. Solid arrows indicate the positions of the acoustic Josephson plasma modes. The coupling between the acoustic Josephson plasma mode and the phonon mode of heavy ions (Hg and Ba) produces the additional dip feature indicated by the open arrows.

spectrum an absorption dip feature appears at the resonance frequency,

$$\omega_r = \frac{\omega_p}{\sqrt{\epsilon_\infty + 2\epsilon_m}}, \tag{2}$$

where ω_p denotes the Josephson plasma frequency and ϵ_m = 1.5 denotes the dielectric constant of polyethylene. ϵ_∞ includes the screening effect of all the optical modes higher than ω_r. Although the accurate value is difficult to estimate, ϵ_∞ of multilayered Hg systems should be comparable to that of Hg-1201 (~20). Each spectrum shows a pronounced dip below T_c which shifts to higher frequency with decreasing temperature. ω_r decreases systematically with increasing n: ~110 cm^{-1} for Hg-1212, ~70 cm^{-1} for Hg-1223, 60 cm^{-1} for Hg-1234, and 50 cm^{-1} for Hg-1245. This tendency is probably due to lowering of the average doping level of CuO_2 planes. Note that on the spectrum of Hg-1223 the Josephson plasma mode strongly couples to the phonon mode at 80 cm^{-1}, so ω_r must be larger than the dip frequency. These values are smaller than those for optimally doped YBCO and larger than those for $La_{2-x}Sr_xCuO_4$ (LSCO), and hence the anisotropy of Hg-based cuprates is in between YBCO and LSCO.

IV. DISCUSSION

The squared frequency of the Josephson plasma mode is a measure of the strength of interlayer Josephson coupling.

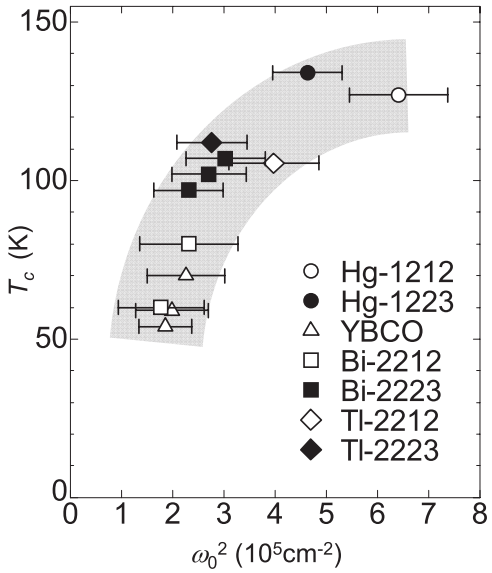

FIG. 5. T_c plotted against the squared optical Josephson plasma frequency for various multilayer cuprates.[15–19] The doping levels for most of the cuprates are near optimal except for YBCO for which the optical mode is clearly seen only in the underdoped regime. In this plot we use the peak frequency of the optical Josephson plasma mode in the reflectivity spectrum ω_0 instead of the edge frequency $\tilde{\omega}_p$.

Figure 5 shows the plot of the squared frequency of the optical Josephson plasma mode ${\omega_0}^2$ at $T = 5$ K against T_c for various bi- and trilayer cuprates.[15–19] A correlation is seen between ω_0^2 and T_c in contrast to the poor correlation between T_c and interlayer Josephson coupling strength in single-layer cuprates.[9,34] We find that the optical Josephson plasma frequencies in Hg-1212 and Hg-1223 with the highest T_c values are the highest among various cuprate superconductors.

Generally, the Josephson coupling strength depends strongly on the distance between two superconducting planes, but the distance between neighboring CuO_2 planes within a multilayer in a Hg-based cuprate is nearly the same as that in other cuprates. In this regard, the intramultilayer Josephson coupling, the Josephson coupling between neighboring CuO_2 planes within a multilayer, in bi- and trilayer Hg-based cuprates is anomalously strong (the plasma frequency $\omega_0 \sim 800$ cm^{-1} for Hg-1212, 480 cm^{-1} for Bi-2212, and 430 cm^{-1} for underdoped YBCO).[15,16] The reason is not clear at the moment, but it is worth noting that T_c correlates with the apical-oxygen distance from the CuO_2 plane, and hence the apical-oxygen distance may correlate with ω_p^2 or Josephson coupling strength (2.8 Å for Hg-1212, 2.4 Å for Bi-2212, and 2.3 Å for YBCO).[35–37]

Now that the intramultilayer Josephson coupling strengths are known, the Josephson coupling energy per unit cell, E_J, can be estimated from the sum of the contribution from possible Josephson junctions formed within a multilayer as

$$E_J = \sum_i \frac{\hbar^2 a^2}{16\pi e^2 d_i} {\omega_{pi}}^2, \tag{3}$$

where d_i denotes the distance between two relevant superconducting planes forming a Josephson junction and a denotes the in-plane lattice constant.[38] Because ${\omega_{pi}}^2$ of the relevant optical mode is much larger than that of the acoustic mode, the Josephson coupling energy E_J is by an order of magnitude larger than that of the intermultilayer Josephson coupling. To estimate E_J, one needs to know the unscreened squared longitudinal optical Josephson plasma frequency ${\omega_p}^2 = \epsilon_\infty \tilde{\omega}_p^2$ ($\tilde{\omega}_p$, the screened plasma frequency). We assume that the high-frequency dielectric constant $\epsilon_\infty = 4$ (from the c-axis reflectivity of Hg-1201) not dependent on n and estimate ω_p's based on the analysis, e.g., as shown in Fig. 3. In the case of $n = 3$, the trilayer is composed of two identical Josephson junctions and hence possesses one optical Josephson plasma mode with E_J twice the contribution from the Josephson junction between the IP and the OP. On the other hand, the multilayers in Hg-1234 and Hg-1245 are a series of inequivalent junctions, two between the IP and the OP and one (two) between the IPs for $n = 4$ ($n = 5$). The higher-frequency mode in $n = 4$ originates from the former junctions, whereas the lower-frequency mode originates from the latter. Thus, E_J for $n = 4$ is given by the sum of the contributions from these three junctions. For Hg-1245 superconducting order parameters in the three IPs would be depressed due to low hole density. As a consequence, the strength of Josephson coupling may be weak, in particular for the coupling between IPs, making the corresponding spectral features weak and shifting to lower frequencies. Although the estimate of the value of ${\omega_p}^2$ is subject to large uncertainty, since the contribution of many phonons (two bending and two Ca modes) overlap, definitely the ${\omega_p}^2$ values are reduced and hence E_J is significantly lower than that for Hg-1234.

As mentioned before, the interlayer Josephson coupling is too weak to account for T_c as high as ~100 K for single-layer cuprates. However, since the intramultilayer Josephson coupling turns out to have substantial strength, it is a possible driving force to enhance T_c in the multilayer structure with respect to T_c of the single-layer material in which different but as yet unresolved pairing interactions give rise to $T_c \sim 100$ K. To check this possibility we plot, in Fig. 6, the intramultilayer Josephson coupling energy per unit cell and per plane, the sum of E_J divided by n, against the increase of T_c of the n-layer compound with respect to the monolayer Hg-1201 [$T_c(1) = 97$ K], $\Delta T_c \equiv T_c(n) - T_c(1)$. One can see that ΔT_c remarkably correlates with the intramultilayer Josephson coupling energy. This indicates that the above scenario is possibly valid to explain the enhancement of T_c of multilayer cuprates, whatever the pairing mechanism which drives T_c to ~100 K is in the single-layer Hg-1201. For most optimally doped cuprates, the superconducting condensation energy U_0 is an order of ~5 K per unit cell per plane.[9,39,40] The estimated value of E_J/n is a substantial fraction of U_0.

Recently, Dordevic *et al.* proposed an alternative interpretation of the c-axis spectrum of underdoped YBCO, in which the 400 cm^{-1} optical mode originates from bilayer splitting; therefore, one might suspect that the observed superconducting responses on the c-axis spectra of the Hg-based cuprates also come from bilayer splitting.[20] However, the strong temperature dependencies below T_c indicate that the origin of these modes

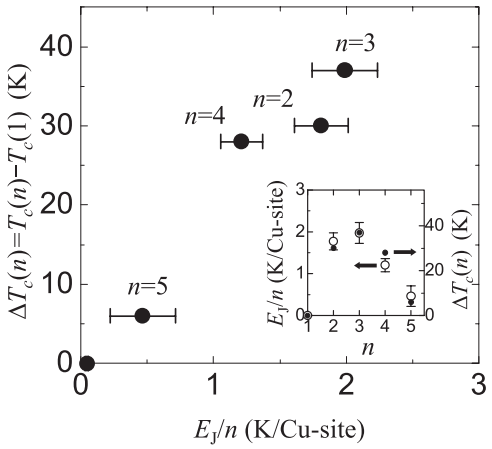

FIG. 6. The relation between Josephson coupling energy per plane (defined in the text) and the change of T_c with respect to T_c of the single-layer system. In the inset both quantities are plotted as a function of n.

is the optical plasma of the superconducting pairs rather than the band structure.

As seen in Figs. 2 and 6 (inset), ω_0 and E_J decrease for n greater than 3. The weakening of the Josephson coupling within a multilayer is apparently related to the doping imbalance between the IP and the OP. If the Josephson coupling strength could be recovered to the level of the bilayer system by reducing the doping imbalance, T_c would go up to above ~150 K for $n = 3$ and above ~170 K for $n = 4$ according to the empirical relationship in Fig. 6. It is speculated that this would happen upon applying high pressure and would partly be responsible for the recorded $T_c = 164$ K at 30 GPa.[41]

V. CONCLUSION

In summary, we have measured the superconducting optical response of polycrystalline samples of Hg-based multilayered cuprates, and the optical Josephson plasma modes arising from intramultilayer Josephson couplings have been successfully observed. The plasma mode is found at frequencies as high as 800 cm^{-1} for bilayer Hg-1212, and its frequency decreases with increasing n for $n \geqslant 3$, reflecting weaker intramultilayer Josephson coupling which appears to be linked to the increasing doping imbalance between the IP and the OP. The highest frequency among the known cuprates may be related with the highest T_c realized in the Hg-based cuprate. We found the intramultilayer Josephson coupling energy well correlates with the increase of T_c with respect to T_c of the monolayer material, which suggests a possibility for further enhancement of T_c for the multilayer system by, for example, reducing the doping imbalance.

ACKNOWLEDGMENTS

We are grateful to N. Bontemps and D. Munzar for helpful discussions. This work was supported by a Grant-in-Aid for Scientific Research from the Ministry of Science and Education (Japan) and the Global COE Program from the Japan Society for the Promotion of Science.

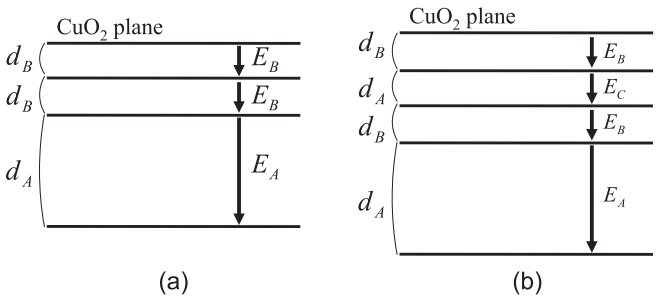

FIG. 7. The schematic pictures of (a) Hg-1223 and (b) Hg-1234. E_A denotes the electric field in the blocking layer, E_B denotes the electric field in the intramultilayer region between the OP and the IP, and E_C denotes the electric field in the intramultilayer region between IPs.

APPENDIX

In order to reproduce the optical spectra of Hg-1223 and Hg-1234 we used the electrostatic model used by Munzar *et al.*[29,30] In this model the ions in crystal are regarded as planes spreading infinitely along the a axis and the b axis, and ions and plasmons produce depolarization fields in response to the local electric fields which are defined in every region separated with CuO_2 planes (Fig. 7). Here we show the parameters for simulation and their definitions (Tables I and II).

1. Model of Hg-1223

In this frequency range between 400 and 700 cm^{-1} the apical-oxygen phonon mode and intramultilayer Josephson plasma mode are important. The electric field of the blocking layer E_A is represented as

$$E_A = E' - \frac{\chi_a}{x_A \epsilon_\infty} E_A. \tag{A1}$$

The first term of the right-hand side E' denotes the external field. The second term represents the depolarization field of the apical-oxygen phonon mode: $\chi_a = S_a/(\omega_a^2 - \omega^2 - i\gamma_a\omega)$ denotes the susceptibility of the apical-oxygen phonon mode. $x_A = d_A/(d_A + 2d_B)$ is the volume fraction of the blocking layer, where d_A and d_B denote the interval lengths between the CuO_2 planes across the blocking layer and the Ca layer, respectively. We assume that the high-frequency dielectric constant $\epsilon_\infty = 4$ (from the c-axis reflectivity of Hg-1201) does not depend on the number of CuO_2 planes n. The electric field of the intramultilayer region E_B is represented as

$$E_B = E' + \frac{1}{\epsilon_\infty}\left(\frac{\omega_p^2}{\omega^2} - i\frac{\sigma_B}{\omega}\right) E_B. \tag{A2}$$

TABLE I. Parameters for reproducing the spectrum of Hg-1223.

ϵ_∞	d_A	d_B	ω_a	S_a	γ_a	ω_p	σ_B
4	9.63	3.16	620	90 000	10	0	3600
4	9.63	3.16	620	90 000	10	1600	400

TABLE II. Parameters for reproducing the spectrum of Hg-1234.

ϵ_∞	d_A	d_B	d_C	ω_a	S_a	γ_a	ω_o	S_o	γ_o	α_{oA}	α_{oB}	α_{oC}	β_{Ao}	β_{Bo}	β_{Co}	ω_{pB}	σ_B	ω_{pC}	σ_C
4	9.37	3.17	3.22	620	90 000	10	390	48 400	24	0.9	0.05	0.05	0.9	0.05	0.05	0	2800	0	2800
4	9.37	3.17	3.22	620	90 000	10	390	48 400	24	0.9	0.05	0.05	0.9	0.05	0.05	1280	200	960	600

The second term of the right-hand side represents the screening field of intramultilayer Josephson plasmons, where ω_p denotes the Josephson plasma frequency of the intramultilayer Josephson junction, and σ_B denotes the background conductivity which controls the damping of the plasma mode. The c-axis dielectric function ϵ is represented as

$$\epsilon = \epsilon_\infty \frac{E'}{E}, \tag{A3}$$

where $E = x_A E_A + x_B E_B$ denotes the average electric field and $x_B = 2d_B/(d_A + 2d_B)$ denotes the volume fraction of the intramultilayer region.

2. Model of Hg-1234

The electric field of the blocking layer, E_A; the intramultilayer region between the OP and the IP, E_B; and the intramultilayer region between IPs, E_C, are represented as

$$E_A = E' - \frac{1}{x_A \epsilon_\infty}\left(\chi_a E_A + \beta_{Ao} P_o\right), \tag{A4}$$

$$E_B = E' + \frac{1}{\epsilon_\infty}\left(\frac{\omega_{pB}^2}{\omega^2} - i\frac{\sigma_B}{\omega}\right) E_B - \frac{\beta_{Bo} P_o}{x_B \epsilon_\infty}, \tag{A5}$$

$$E_C = E' + \frac{1}{\epsilon_\infty}\left(\frac{\omega_{pC}^2}{\omega^2} - i\frac{\sigma_C}{\omega}\right) E_C - \frac{\beta_{Co} P_o}{x_C \epsilon_\infty}, \tag{A6}$$

and the polarization of the out-of-phase bending phonon mode P_o is represented as

$$P_o = \chi_o(\alpha_{oA} E_A + \alpha_{oB} E_B + \alpha_{oC} E_C), \tag{A7}$$

where $x_A = d_A/(d_A + 2d_B + d_C)$, $x_B = 2d_B/(d_A + 2d_B + d_C)$, and $x_C = d_C/(d_A + 2d_B + d_C)$. ω_{pB} denotes the Josephson plasma frequency of the Josephson junction between the OP and the IP, and ω_{pC} denotes the Josephson plasma frequency of the Josephson junction between IPs. $\chi_o = S_o/(\omega_o^2 - \omega^2 - i\gamma_o\omega)$ denotes the susceptibility of the out-of-phase bending phonon mode. The parameters α_{oA}, α_{oB}, and α_{oC} show how much the out-of-phase bending phonon mode feels E_A, E_B, and E_C, respectively. β_{Ao}, β_{Bo}, and β_{Bo} show how much the polarization of the out-of-phase bending phonon mode contribute to E_A, E_B, and E_C, respectively.

[1] Y. J. Uemura, G. M. Luke, B. J. Sternlieb, J. H. Brewer, J. F. Carolan, W. N. Hardy, R. Kadono, J. R. Kempton, R. F. Kiefl, S. R. Kreitzman, P. Mulhern, T. M. Riseman, D. Ll. Williams, B. X. Yang, S. Uchida, H. Takagi, J. Gopalakrishnan, A. W. Sleight, M. A. Subramanian, C. L. Chien, M. Z. Cieplak, Gang Xiao, V. Y. Lee, B. W. Statt, C. E. Stronach, W. J. Kossler, and X. H. Yu., Phys. Rev. Lett. **62**, 2317 (1989).

[2] E. Pavarini, I. Dasgupta, T. Saha-Dasgupta, O. Jepsen, and O. K. Andersen, Phys. Rev. Lett. **87**, 047003 (2001).

[3] B. A. Scott, E. Y. Suard, C. C. Tsuei, D. B. Mitzi, T. R. McGuire, B.-H. Chen, and D. Walker, Physica C **230**, 239 (1994).

[4] A. Iyo, Y. Tanaka, Y. Kodama, H. Kito, K. Tokiwa, and T. Watanabe, Physica C **445-448**, 17 (2006).

[5] For example, P. W. Anderson, Science **268**, 1154 (1995).

[6] S. Chakravarty, Eur. Phys. J. B **5**, 337 (1998).

[7] A. J. Leggett, Phys. Rev. Lett. **83**, 392 (1999).

[8] A. A. Tsvetkov, D. van der Marel, K. A. Moler, J. R. Kirtley, J. L. de Boer, A. Meetsma, Z. F. Ren, N. Koleshnikov, D. Dulic, A. Damascelli, M. Grüninger, J. Schützmann, J. W. van der Eb, H. S. Somal, and J. H. Wang, Nature (London) **395**, 360 (1998).

[9] J. R. Kirtley, K. A. Moler, G. Villard, and A. Maignan, Phys. Rev. Lett. **81**, 2140 (1998).

[10] H. Kotegawa, Y. Tokunaga, K. Ishida, G.-q Zheng, Y. Kitaoka, K. Asayama, H. Kito, A. Iyo, H. Ihara, K. Tanaka, K. Tokiwa, and T. Watanabe, J. Phys. Chem. Solids **62**, 171 (2001).

[11] H. Kotegawa, Y. Tokunaga, Y. Araki, G.-q. Zheng, Y. Kitaoka, K. Tokiwa, K. Ito, T.Watanabe, A. Iyo, Y. Tanaka, and H. Ihara, Phys. Rev. B **69**, 014501 (2004).

[12] S. Chakravarty, H.-Y. Kee, and K. Völker, Nature (London) **428**, 53 (2004).

[13] K. Tamasaku, Y. Nakamura, and S. Uchida, Phys. Rev. Lett. **69**, 1455 (1992).

[14] D. van der Marel and A. A. Tsvetkov, Czech. J. Phys. **46**, 3165 (1996).

[15] C. C. Homes, T. Timusk, R. Liang, D. A. Bonn, and W. N. Hardy, Phys. Rev. Lett. **71**, 1645 (1993).

[16] V. Železný, S. Tajima, D. Munzar, T. Motohashi, J. Shimoyama, and K. Kishio, Phys. Rev. B **63**, 060502(R) (2001).

[17] A. V. Boris, D. Munzar, N. N. Kovaleva, B. Liang, C. T. Lin, A. Dubroka, A. V. Pimenov, T. Holden, B. Keimer, Y.-L. Mathis, and C. Bernhard, Phys. Rev. Lett. **89**, 277001 (2002).

[18] K. F. Renk, W. Ose, T. Zetterer, J. Schützmann, H. Lengfellner, H. H. Otto, J. Keller, B. Roas, L. Schultz, and G. Saemann-Ischenko, Infrared Phys. **29**, 791 (1989).

[19] T. Zetterer, M. Franz, J. Schutzmann, W. Ose, H. H. Otto, and K. F. Renk, Phys. Rev. B **41**, 9499 (1990).

[20] S. V. Dordevic, E. J. Singley, J. H. Kim, M. B. Maple, S. Komiya, S. Ono, Y. Ando, T. Rõõm, R. Liang, D. A. Bonn, W. N. Hardy, J. P. Carbotte, C. C. Homes, M. Strongin, and D. N. Basov, Phys. Rev. B **69**, 094511 (2004).

[21]M. Hirabayashi, K. Tokiwa, M. Tokumoto, and H. Ihara, Jpn. J. Appl. Phys. **32**, L1206 (1993).
[22]K. Tokiwa, A. Iyo, T. Tsukamoto, and H. Ihara, Czech. J. Phys. **46**, 1491 (1996).
[23]C. W. Chu, IEEE Trans. Appl. Supercond. **7**, 80 (1997).
[24]E. V. Antipov, A. M. Abakumov, and S. N. Putilin, Supercond. Sci. Technol. **15**, R31 (2002).
[25]D. Stroud, Superlattices Microstruct. **23**, 567 (1998).
[26]J. J. McGuire, M. Windt, T. Startseva, T. Timusk, D. Colson, and V. Viallet-Guillen, Phys. Rev. B **62**, 8711 (2000).
[27]T. W. Noh, S. G. Kaplan, and A. J. Sievers, Phys. Rev. B **41**, 307 (1990).
[28]E. van Heumen, R. Lortz, A. B. Kuzmenko, F. Carbone, D. van der Marel, X. Zhao, G. Yu, Y. Cho, N. Barisic, M. Greven, C. C. Homes, and S. V. Dordevic, Phys. Rev. B **75**, 054522 (2007).
[29]D. Munzar, C. Bernhard, A. Golnik, J. Humlíček, and M. Cardona, Solid State Commun. **112**, 365 (1999).
[30]A. Dubroka and D. Munzar, Physica C **405**, 133 (2004).
[31]A. Sacuto, R. Combescot, N. Bontemps, C. A. Muller, V. Viallet, and D. Colson, Phys. Rev. B **58**, 11721 (1998).
[32]It is known for YBCO that the frequency of the optical Josephson mode decreases with decreasing doping concentration in the CuO_2 plane. See S. Tajima, J. Schutzmann, S. Miyamoto, I. Terasaki, Y. Sato, and R. Hauff, Phys. Rev. B **55**, 6051 (1997).
[33]Z. A. Xu, N. P. Ong, Y. Wang, T. Kakeshita, and S. Uchida, Nature (London) **406**, 486 (2000).
[34]J. Schützmann, H. S. Somal, A. A. Tsvetkov, D. van der Marel, G. E. J. Koops, N. Koleshnikov, Z. F. Ren, J. H. Wang, E. Bruck, and A. A. Menovsky, Phys. Rev. B **55**, 11118 (1997).
[35]M. Cantoni, A. Schilling, H.-U. Nissen, and H. R. Ott, Physica C **215**, 11 (1993).
[36]R. E. Gladyshevskii and R. Flükinger, Acta Crystallogr. Sect. B **52**, 38 (1996).
[37]J. D. Jorgensen, B. W. Veal, A. P. Paulikas, L. J. Nowicki, G. W. Crabtree, H. Claus, and W. K. Kwok, Phys. Rev. B **41**, 1863 (1990).
[38]D. Munzar, C. Bernhard, T. Holden, A. Golnik, J. Humlicek, and M. Cardona, Phys. Rev. B **64**, 024523 (2001).
[39]J. W. Loram, K. A. Mirza, J. M. Wade, J. R. Cooper, and W. Y. Liang, Physica C **235-240**, 134 (1994).
[40]J. W. Loram, J. L. Luo, J. R. Cooper, W. Y. Liang, and J. L. Tallon, Physica C **341-348**, 831 (2000).
[41]C. W. Chu, L. Gao, F. Chen, Z. J. Huang, R. L. Meng, and Y. Y. Xue, Nature (London) **365**, 323 (1993).